# Observation of Lie algebraic invariants in quantum linear optics

Giovanni Rodari,[1] Tommaso Francalanci,[1] Eugenio Caruccio,[1] Francesco Hoch,[1] Gonzalo Carvacho,[1] Taira Giordani,[1] Nicolò Spagnolo,[1] Riccardo Albiero,[2] Niki Di Giano,[2,3] Francesco Ceccarelli,[2] Giacomo Corrielli,[2] Andrea Crespi,[2,3] Roberto Osellame,[2] Ulysse Chabaud,[4] and Fabio Sciarrino[1,*]

[1]*Dipartimento di Fisica, Sapienza Università di Roma, Piazzale Aldo Moro 5, I-00185 Roma, Italy*

[2]*Istituto di Fotonica e Nanotecnologie, Consiglio Nazionale delle Ricerche (IFN-CNR), Piazza Leonardo da Vinci 32, I-20133 Milano, Italy*

[3]*Dipartimento di Fisica—Politecnico di Milano, Piazza Leonardo da Vinci 32, 20133 Milano, Italy*

[4]*DIENS, École Normale Supérieure, PSL University, CNRS, INRIA, 45 rue d'Ulm, 75005 Paris, France*

(Received 19 May 2025; accepted 1 December 2025; published 22 December 2025)

Over the past few years, various methods have been developed to engineer and to exploit the dynamics of photonic quantum states as they evolve through linear optical networks. Recent theoretical works have shown that the underlying Lie algebraic structure plays a crucial role in the description of linear optical Hamiltonians, as such formalism identifies intrinsic symmetries within photonic systems subject to linear optical dynamics. Here, we experimentally investigate the role of Lie algebras applied to the context of Boson sampling, a pivotal model to the current understanding of computational complexity regimes in photonic quantum information. Performing experiments of increasing complexity, realized within a fully reconfigurable photonic circuit, we show that sampling experiments do indeed fulfill the constraints implied by a Lie algebraic structure. In addition, we provide a comprehensive picture about how the concept of Lie algebraic invariant can be interpreted from the point of view of *n*th-order correlation functions in quantum optics. Our work shows how Lie algebraic invariants can be used as a benchmark tool for the correctness of an underlying linear optical dynamics within typical interferometric architectures for photonic quantum information. This opens avenues for the use of algebraic-inspired methods as analysis tools for photon-based quantum computing protocols.

DOI: 10.1103/7961-hg2q

## I. INTRODUCTION

Harnessing linear optical systems has been a cornerstone of photonic-based quantum information processing, finding several applications [1–5]. In particular, boson sampling and its variants [6–12] have been proposed as a model in which multiphoton states, linear optical evolution, and subsequent photon detection can be employed to reach the quantum advantage regime [13,14] with current photonic technologies [15–17]. Research efforts in this paradigm have been stimulated by its suitability to observe the enhanced computational power of quantum devices for solving a classically hard problem [6], and by the development of photon-based universal quantum computation schemes [18,19]. As demonstrated in increasingly complex schemes [20–32], boson sampling photonic platforms provide a suitable test bed to investigate approaches to analyze quantum computational complexity. In this context, several benchmarking methods have been proposed to quantitatively assess the correct functioning of such quantum devices [33–42].

Recently, concepts stemming from Lie algebras theory have been proposed as tools for quantum computing [43] and for the analysis and design of photonics-based quantum information protocols reliant on linear optics [44–46]. In this framework, the mathematical toolbox describing how photon states evolve within a linear optical network—e.g., scattering matrices or unitary operators acting on Fock-basis states—is approached via Lie algebras, providing an alternative description of linear optical transformations. This parallel offers an insight into the dynamics of quantum linear optical evolutions without the need of devising particularly complex measurement setups, i.e., many-mode interactions. Specifically, one can identify Lie algebraic invariants—measurable quantities that are conserved under linear optical transformations—which characterize photonic evolution [44]. Due to considerations connected to the theory of Lie algebra, the value of a suitably constructed function of expectation values measured at the output of an optical circuit is conserved whenever the underlying dynamic is linear. Operationally, the lowest order invariants can be computed by measuring the mean photon numbers on a given set of outputs of a linear optical network, or their combination after further manipulation in order to implement two-mode operators. These objects are instrumental in defining particular constraints and symmetries that do characterize the behavior of linear-based

*Contact author: fabio.sciarrino@uniroma1.it

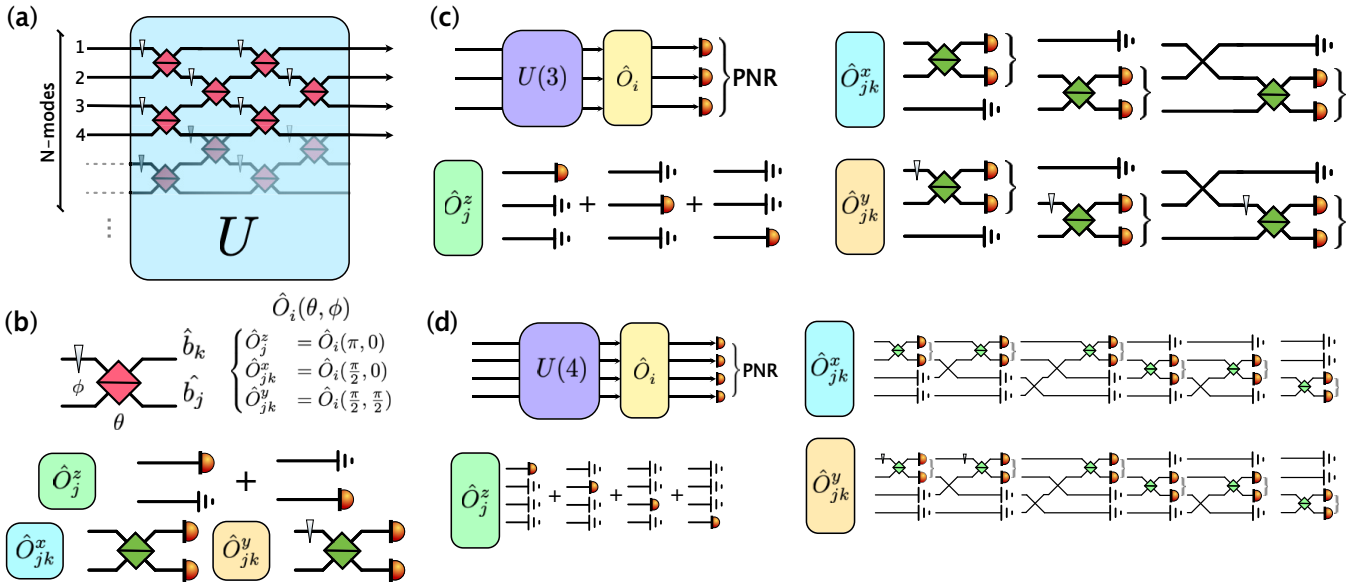


FIG. 1. Linear optical schemes for measuring Lie algebraic invariants: (a) An $m$-mode unitary transformation constructed only via linear optical elements, variable beam splitters (red squares), and phase shifters (light blue triangles) is provided together with an arbitrary photon input state, $\rho$, with $\rho = |\boldsymbol{s}\rangle\langle\boldsymbol{s}|$. In our experiment, $|\boldsymbol{s}\rangle$ denotes a multimode $n$-photon Fock state. The state evolves throughout the interferometer, leading to an output state $\rho'$. (b) In order to measure the invariant $I(\rho')$, as defined in Eq. (2), on the state $\rho'$ at the output of a linear optical dynamic, every possible pair of output modes is let interfere through optical setups involving at most two modes, as depicted in the panel, through which the expectation values of the operators $\{O^z_j, O^x_{jk}, O^y_{jk}\}$ on state $\rho'$ can be measured. Here, the green square denotes a variable beam splitter set to a 50:50 splitting ratio. (c) The unitary transformation $U(3)$ is followed by a mode-swapping setup and the circuits shown in panel (b) in order to measure the expectation values of a given operator, which requires photon number resolving detection. In this way, the experimental value of the invariant $I(\rho')$ in the $m = 3$ scenario can be reconstructed. (d) Similarly, the experimental value of the invariant $I(\rho)$ in the $m = 4$ scenario can be reconstructed by implementing jointly a linear optical transformation represented by a unitary matrix $U(4)$ followed by the measurement setups required to probe the aforementioned expectation values. Also in this case, photon-number resolving detection is operated at the output.

photonic systems, i.e., the framework of boson sampling. In particular, this provides a perspective on the constraints imposed by linear optics on the accessible output states. This is particularly relevant in the context of boson sampling, where characterizing the set of reachable distributions helps in assessing its potential for quantum computing applications, such as quantum machine learning in its adaptive variant [11,32].

In this article, we experimentally investigate the role of invariants of the Lie algebra of linear-optics Hamiltonians within the context of boson sampling. We explore how these invariants can be measured and verified using a state-of-the-art photonic architecture. We validate the feasibility of measuring such quantities in photonic experiments of increasing size, employing up to four-photon states obtained via a demultiplexed quantum dot source [15,47,48] and injected in an eight-mode, fully reconfigurable photonic circuit [49–52]. We are able to accurately program the interferometer to implement a controlled linear optical evolution followed by a set of photon number measurements, required to experimentally estimate a given Lie algebraic quantity. In addition, we show how the operators and invariant quantities of the Lie algebra can be connected to the concepts of quantum correlations and coherence properties of quantum states of light. Overall, we provide an insight into the role of Lie algebraic tools in the theoretical understanding and experimental implementations of linear optical dynamics within the context of photon-based quantum information processing.

## II. BACKGROUND: THE ROLE OF LIE ALGEBRAIC INVARIANTS IN LINEAR OPTICS

The dynamical behavior of photonic quantum states undergoing a general linear optical evolution was characterized, from the point of view of quantum state preparation, in a recent work by Parellada, *et al.* [44]. By exploiting the connection between the unitary evolution generated by a passive linear optical interferometer and the mathematical structure of Lie algebras [46], several invariant quantities are derived for passive linear optical systems. Such invariants, all stemming from the projection of the density operator describing the quantum states onto the Lie algebra of passive linear optical Hamiltonians, are conserved when a quantum state evolves through a passive linear optical interferometer.

Conserved quantities arise when one considers the expectation values over a suitable operator basis describing the algebraic space of linear optical Hamiltonian operators. In particular, the following basis of Hermitian operators, namely, physical observables, can be adopted for a system characterized by $m$ optical modes as in Fig. 1(a):

$$O^z_j = n_j = a^\dagger_j a_j, \qquad \text{for } j = 1,\ldots,m,$$

$$O^x_{jk} = \frac{1}{\sqrt{2}}(a^\dagger_j a_k + a^\dagger_k a_j), \quad \text{for } 1 \leqslant j < k \leqslant m,$$
$$O^y_{jk} = \frac{i}{\sqrt{2}}(a^\dagger_j a_k - a^\dagger_k a_j), \quad \text{for } 1 \leqslant j < k \leqslant m. \tag{1}$$

The expectation values of the observables in Eq. (1) can be experimentally measured, with multimode interferometers, in the following way: (1) for the $O^z_j$ operators, by probing the populations of the output density matrix expressed in the Fock basis representation and (2) for the operators $O^{x,y}_{jk}$, by measuring the mean photon number difference $\langle n_j\rangle - \langle n_k\rangle$ between modes $j$ and $k$ [53] after letting two modes $(j,k)$ interfere on a balanced beam splitter, with an additional phase term set to 0 ($\frac{\pi}{2}$) for $O^x_{jk}$ ($O^y_{jk}$). The schemes to measure such operators for two spatial modes are shown in Fig. 1(b). The construction can be generalized to a higher number of modes, as shown for three (four) spatial modes in Fig. 1(c) [Fig. 1(d)], where additional mode swapping is required to correctly let modes $(j,k)$ interfere. Note that, at variance from a standard boson sampling experiment, the measurement of the observables defined above also requires an additional measurement stage after the linear optical evolution, as depicted in Fig. 1. Moreover, the adopted detectors should have the capability to resolve the number of photons on each detected mode in order to compute the required mean photon number values $\langle n_k\rangle$.

### A. Lie algebraic invariants of interest

The first Lie algebraic invariant of interest is obtained as the sum of the squared expectation values of the observables defined in Eq. (1):

$$I(\rho) = \sum_{i=1}^{m^2} \mathrm{Tr}(O_i\rho)^2. \tag{2}$$

This scalar quantity represents the purity of the state projected onto the chosen basis and remains unchanged under linear optical evolution. Considering as input a fixed generic Fock state $|\boldsymbol{s}\rangle = |n_1, ..., n_m\rangle$ comprising $n = \sum_{j=1}^m n_j$ photons traversing $m$ optical modes, it can be shown that

$$I(|s\rangle\langle s|) = \sum_{j=1}^{m} n_j^2. \tag{3}$$

Notably, for Fock basis pure states comprising $n$ photons distributed in such a way to exhibit at most one photon per mode—i.e., the prototypical input state employed in several recent demonstrations of photon-based quantum information protocols—Eq. (3) reduces to $I(|s\rangle\langle s|) = n$. Since the expectation values $\mathrm{Tr}(O_i\rho)$ are experimentally measurable with the apparatus shown in Fig. 1, one can directly test whether $I(\rho)$ is conserved for a given input state after optical evolution. If this quantity is not conserved, one should conclude that the evolution is nonlinear. Moreover, if two states have different values of $I(\rho)$, they cannot be connected by a passive linear optical transformation.

A second Lie algebraic invariant can be obtained considering the infinite-dimensional density operator defined as

$$\rho_T = \sum_{i=1}^{m^2} \mathrm{Tr}(O_i\rho)O_i. \tag{4}$$

The operator $\rho_T$ represents the projection of the density matrix onto the subalgebra of linear optical Hamiltonians. The eigenvalue spectrum of $\rho_T$ is indeed invariant under linear optical evolution. The invariance of its spectrum follows from the fact that linear optical evolution keeps it within the subalgebra, as shown in Ref. [44]. Note that the spectrum of $\rho_T$ has infinite cardinality and, since $\rho_T$ preserves the total number of photons, it is block diagonal. In what follows, we will refer to the eigenvalues of each block as $\lambda_n$, with $n$ being the conserved number of photons of each block (see the Supplemental Material [54] for more details). This result provides additional constraints beyond $I(\rho)$, as it gives more information than a single scalar value. The previous physical invariants provide valuable tools for analyzing the possibilities and limitations of state preparation in quantum linear optics. Indeed, they help to constrain the search for the linear unitary evolution preparing a given output photon state, which might be impossible to obtain due to the nonconservation of the associated invariant with respect to a fixed input resource.

### B. Connection with the concept of quantum optical coherency matrix

An interesting insight into the physical meaning of the observables in Eq. (1) can be gained by recalling the concept of quantum optical coherency matrix [55,56], an $m \times m$ square matrix with entries:

$$(\mathbf{\Gamma}^{(1)})_{jk} = \langle a^\dagger_j a_k\rangle. \tag{5}$$

Such entries are in fact proportional to the first-order quantum correlation functions for the multimode field $G^{(1)}_{jk} = \langle E^-_j E^+_k\rangle \propto \langle a^\dagger_j a_k\rangle$. The quantum coherency matrix is Hermitian, and may be written more compactly as

$$\mathbf{\Gamma}^{(1)} = \langle \vec{a}^\dagger \vec{a}^T\rangle, \tag{6}$$

where $\vec{a}$ is a column vector containing the annihilation operators of the $m$ modes. The entries of the coherency matrix are related to the expectation values of the observables (1) by the following linear transformations:

$$(\mathbf{\Gamma}^{(1)})_{jk} = (\mathbf{\Gamma}^{(1)})^*_{kj} = \frac{1}{\sqrt{2}}\left(\langle O^x_{jk}\rangle - i\langle O^y_{jk}\rangle\right),$$
$$(\mathbf{\Gamma}^{(1)})_{jj} = \langle O^z_j\rangle. \tag{7}$$

Thus, the experimental estimation of the expectation values $\langle O_i\rangle$ coincides with the experimental characterization of the quantum coherency matrix of the multimode field. It can be further noted that the information contained in the operator $\rho_T$ in Eq. (4) is the same contained in the coherency matrix, as we can obtain the coefficients $\langle O_i\rangle = \mathrm{Tr}(O_i\rho)$ from the entries of the coherency matrix and vice versa, using Eq. (7).

The effect of a linear optical transformation on the output coherence matrix is equivalent to a basis change in the representation of $\mathbf{\Gamma}^{(1)}$ [55]. This follows from direct application of the unitary operator that represents a given linear optical transformation to the bosonic operators in the definition of the coherency matrix as in Eqs. (6) and(7). In particular, let $U$ be the unitary matrix describing the linear-optics transformation on the set of creation vectors of the optical modes, so that the equalities $\vec{b}^\dagger = U\vec{a}^\dagger$ and $\vec{b} = U^*\vec{a}$ hold. Then, a linear optical

evolution acts on the coherency matrix as a basis change, according to

$$\mathbf{\Gamma}_b^{(1)} = \langle \vec{b}^\dagger \vec{b}^T \rangle = U \langle \vec{a}^\dagger \vec{a}^T \rangle U^\dagger. \tag{8}$$

The relation between the expectation values $\langle O_i \rangle$ and the entries of the coherency matrix in Eq. (7) allows us to give interesting interpretations of the algebraic invariants discussed above. Noting that $\langle O^x_{jk} \rangle = \sqrt{2}\mathrm{Re}\{\langle a_j^\dagger a_k \rangle\}$ and $\langle O^y_{jk} \rangle = -\sqrt{2}\mathrm{Im}\{\langle a_j^\dagger a_k \rangle\}$, one can easily derive that the quantity $I(\rho)$ in Eq. (2) corresponds to

$$I(\rho) = \sum_{j,k} |\langle a_j^\dagger a_k \rangle|^2 = \sum_{j,k} |(\mathbf{\Gamma}^{(1)})_{jk}|^2 = \mathrm{Tr}[(\mathbf{\Gamma}^{(1)})^\dagger \mathbf{\Gamma}^{(1)}]. \tag{9}$$

Namely, the invariant $I(\rho)$ corresponds to the Frobenius norm of the coherency matrix. Then, the fact that $I(\rho)$ is an invariant for linear-optics transformations directly corresponds to the conservation of the norm of the coherency matrix $\mathbf{\Gamma}^{(1)}$ upon a change of basis.

Furthermore, as the coherency matrix is Hermitian, there is always an eigenvector basis that diagonalizes it, which is the basis of the *principal modes* [55]. The modes as defined in this basis do not show classical interference with each other, because the nondiagonal elements corresponding to the correlations of the operators $G^{(1)}_{jk}$ with $j \neq k$ vanish in this basis. The eigenvalues of the coherency matrix, namely, the diagonal entries when the matrix is diagonalized, are the photon populations $\langle N_i \rangle$ of such principal modes. The value of $I(\rho)$, interpreted as the squared norm of the matrix, equals the sum of the squares of the eigenvalues, i.e., $I(\rho) = \sum_i (\langle N_i \rangle)^2$. This observation allows us to set a simple bound for the values that $I(\rho)$ can take, when comparing different optical states defined over $m$ modes having the same overall photon number $\bar{N}_{tot} = \sum_i \langle N_i \rangle$. It is straightforward to show that the minimum value for the invariant $I(\rho)$ is achieved when we have $m$ principal modes that are equally populated:

$$I(\rho)|_{\min} = \frac{\bar{N}^2_{\mathrm{tot}}}{m}, \tag{10}$$

while the maximum value is achieved in the case of all photons populating a single principal mode:

$$I(\rho)|_{\max} = \bar{N}^2_{\mathrm{tot}}. \tag{11}$$

We note that the eigenvalues of the coherency matrix are naturally conserved upon changes of basis and are therefore invariants in linear-optics transformations. However, not all the possible invariants derived as functions of $\langle O_i \rangle$ are independent. It can be shown, as described in detail in the Supplemental Material [54], that the maximum number of independent invariants that can be obtained is given by $m$. Thus, for a given number of modes $m$ and a given initial state preparation, it is equivalent to check for the invariance of the $m$ eigenvalues of $\mathbf{\Gamma}^{(1)}$ or, for instance, of the quantity $I(\rho)$ plus other $m-1$ independent invariant quantities. Indeed, we show in the Supplemental Material [54] that the information contained in the $m$ eigenvalues of $\mathbf{\Gamma}^{(1)}$ is equivalent to the information provided by the spectrum of the Hermitian operator $\rho_T$ defined in Eq. (4).

As mentioned in Ref. [44], one may not be limited to the construction of functions of $\langle O_i \rangle$, but may exploit also products of operators $O_i$, which potentially allows to increase the number of independent invariants that can be derived. Note that any product of operators $O_i$ can be cast into a linear combination of products of creation and annihilation operators, in equal number, possibly on different modes. Interestingly, one can show that such products are related to $n$th-order quantum correlation functions on a set of modes specified by the indices $(s_1, \ldots, s_n, s_{n+1}, \ldots, s_{2n})$, which can be written in a-dimensional form as

$$\Gamma^{(n)}(s_1, \ldots, s_{2n}) = \left\langle a^\dagger_{s_1} \cdots a^\dagger_{s_n} a_{s_{n+1}} \cdots a_{s_{2n}} \right\rangle. \tag{12}$$

Thus, our discussion on the invariants related to the quantum coherency matrix appears to be a particular case of a more general physical object, in which one considers a $2n$-order tensor having as entries the $n$th-order coherency matrix $\Gamma^{(n)}(s_1, \ldots, s_{2n})$, as discussed in the Supplemental Material [54].

However, the measurement of generic higher-order correlation functions (or related observables) presents increasing experimental challenges, due both to the growing complexity of the experimental setup and the exponential increase in the number of possible measurements—as the components of a $2n$-order tensor scale with $m^{2n}$. For this reason, in the present work, we focus on the experimental investigation of invariants associated with first-order correlations.

## III. EXPERIMENTAL MEASUREMENTS AND VALIDATION OF LIE ALGEBRAIC OBSERVABLES

As described above, the evolution of a photonic state within a linear optical network implies the conservation of specific quantities, which can be derived from an underlying Lie algebraic structure. Moreover, such conservation laws are intrinsically connected to the concept of quantum optical coherency matrices. We now describe how the conservation of the described Lie invariant quantities for $n$photon states evolving through a $m$mode linear optical network has been experimentally verified, by carrying out observations featuring linear optical evolutions of up to $n = 4$ photon states subjected to up to a $m = 4$ mode unitary evolution.

### A. Experimental setup and results

We employ an advanced hybrid photonic architecture tailored for photon-based multiphoton experiments [33,57,58], whose main components for single-photon generation, preparation, and manipulation of multiphoton resources are depicted in Fig. 2. A Quantum Dot (QD) single-photon source [15,47,48,48,59] is paired with a time-to-spatial demultiplexer to obtain a stream of multiphoton states [33,41,57,58,60]. Linear optical evolution is obtained within an eight-mode fully reconfigurable photonic integrated circuit (PIC) fabricated by femtosecond laser waveguide writing in glass [49]. The precise reconfigurability of the interferometer is obtained via calibration [51] of the thermo-optic shifters fabricated on the device surface [61]. In the experiment, the PIC is set to implement a known unitary transformation $U$ followed by the required measurement operators $O_{ij}$. We test Lie algebraic invariants with unitary transformations requiring up to $m = 4$ modes within our $M = 8$ modes PIC. Thus, we employ

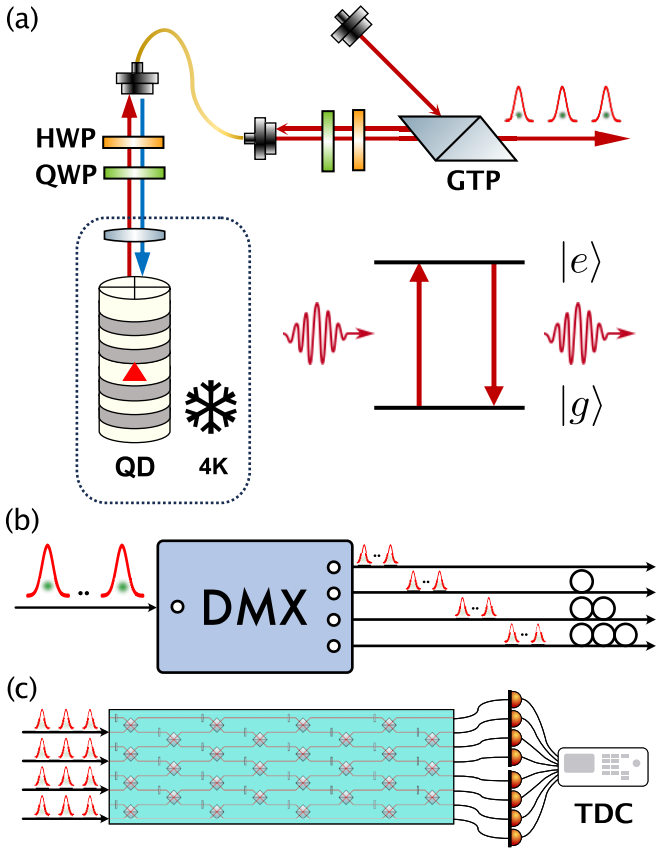


FIG. 2. The employed state-of-the-art hybrid photonic architecture: (a) A quantum-dot (QD) single-photon source is resonantly excited in a cross-polarized configuration where separation of the residual pump laser is achieved by means of a Glan-Thompson polarizer, half-wave plates, and quarter-wave plates, to compensate from the polarization rotations induced by the propagation in the optical fiber and control the laser pump polarization state at the interface with the QD. (b) A time-to-spatial demultiplexer actively splits the input single-photon stream into a fixed set of output modes, where a multiphoton resource state with up to $n = 4$ photons is obtained. (c) The time-to-space demultiplexed source is interfaced with an eight-mode, fully reconfigurable photonic integrated circuit. Here, the circuit is programmed in such a way to implement a linear optical dynamic followed by the optical setup required to measure the Lie operators, as shown in Fig. 1. At the output of the circuit, photon detection is carried out via superconducting nanowire detectors, connected a time-to-digital converter, which records $n$-fold coincidence events. Legend: Glan-Thompson polarizer (GTP), half-wave plate (HWP), quarter-wave plate (QWP), time-to-digital converter (TDC).

the first $m$ layers of the device by setting the corresponding $m(m-1)$ phases to implement a random unitary transformation in $SU(m)$, following the scheme in Ref. [52]. Given that only $m$ layers are needed to achieve this, we utilize the remaining $(M-m)$ layers to implement the transformations required in order to measure the expectation values of the observables $O_i$ of Fig. 1. This is accomplished through the action of balanced beam splitters and cross beam splitters, swapping two spatial modes, as shown in Figs. 1(c) and 1(d) for both the $m = 3$ and $m = 4$ configurations. To reconstruct the expectation values of the observables, we determine the probability amplitudes for all possible photon-number outcomes, including those where multiple photons exit the linear interferometer bunching in the same mode, with pseudo-photon-number-resolving techniques. Specifically, at each output mode of the linear interferometer, we insert a suitably constructed cascade of balanced beam splitters, implemented both on-chip and externally via in-fiber beam splitter. In such a way, we can probe the full output photon-number distribution by correcting the measured $n$-fold coincidence events with a numerical factor taking into account the conditional probability of successful detection of a bunching event and the detector efficiencies, as detailed in the Supplemental Material [54].

We performed measurements of the output photon number distributions for several different experimental configurations, in terms of both the number of photons $n$ injected in the integrated chip and the number of modes $m$, which determine the dimension of the addressed linear-optical unitary transformation. Moreover, the initial state injected in the PIC, expressed in the Fock-basis space, features at most one photon per input mode. For each configuration $\{n, m\}$, we randomly extracted (with respect to the Haar-random measure) about 100 linear optical unitary transformation that were mapped onto phase settings to program the PIC so-called square decomposition algorithm [52].

### B. Invariance of the algebraic quantity $I(\rho)$

We first tested the Lie algebraic invariant of Eq. (2) across various boson sampling configurations, with varying number of photons $n$ and modes $m$, up to $n = m = 4$ (see Fig. 3). In each of them, we chose different no-collision Fock state inputs in the form $|1^{\otimes n}0^{\otimes(m-n)}\rangle$; while implementing Haar-random unitary transformations $SU(m)$. The expectation values of the observables in Eq. (1) were derived using the reconstructed populations of the output state, as detailed in the Supplemental Material [54]. From them, the quantity $I(\rho)$ can be computed. We note that in the experiment we only record $n$-photon coincidences, i.e., events in which the number of detected photons is equal to the number of photons injected in the interferometer. Therefore, balanced optical losses equally impact all the detection events considered to reconstruct the output photon number distribution and can be disregarded.

The distributions of the experimentally probed values of the quantity $I(\rho)$, amongst a large number of Haar-random unitary evolutions and for different numbers of photons $n$ and modes $m$, are shown in Fig. 3(a). Furthermore, to evaluate the accuracy of the population reconstruction, we performed numerical simulations of the experiments for a given output state $\rho$, we employ the metric $1 - \mathrm{TD}_{\mathrm{sim}}$, where $\mathrm{TD}_{\mathrm{sim}}$ denotes the trace distance from the corresponding simulated output state $\rho_{\mathrm{sim}}$, calculated as $\mathrm{TD}_{\mathrm{sim}} = \frac{1}{2}\mathrm{Tr}|\rho - \rho_{\mathrm{sim}}|$. In Table I, we present the averaged values of $1 - \mathrm{TD}_{\mathrm{sim}}$, across all unitary transformations and observables. Additionally, Table I displays the average measured value of $I(\rho)$ and its associated standard deviation computed across all the dialled unitary evolution for all $\{n, m\}$ configurations. Note that, in each scenario, we obtain average values of $I_{\mathrm{exp}}(\rho)$, which are compatible, within two standard deviations, with the theoretically expected value being $I(\rho) = n$, as proven in the Supplemental Material [54]. We also note that a small deviation between the

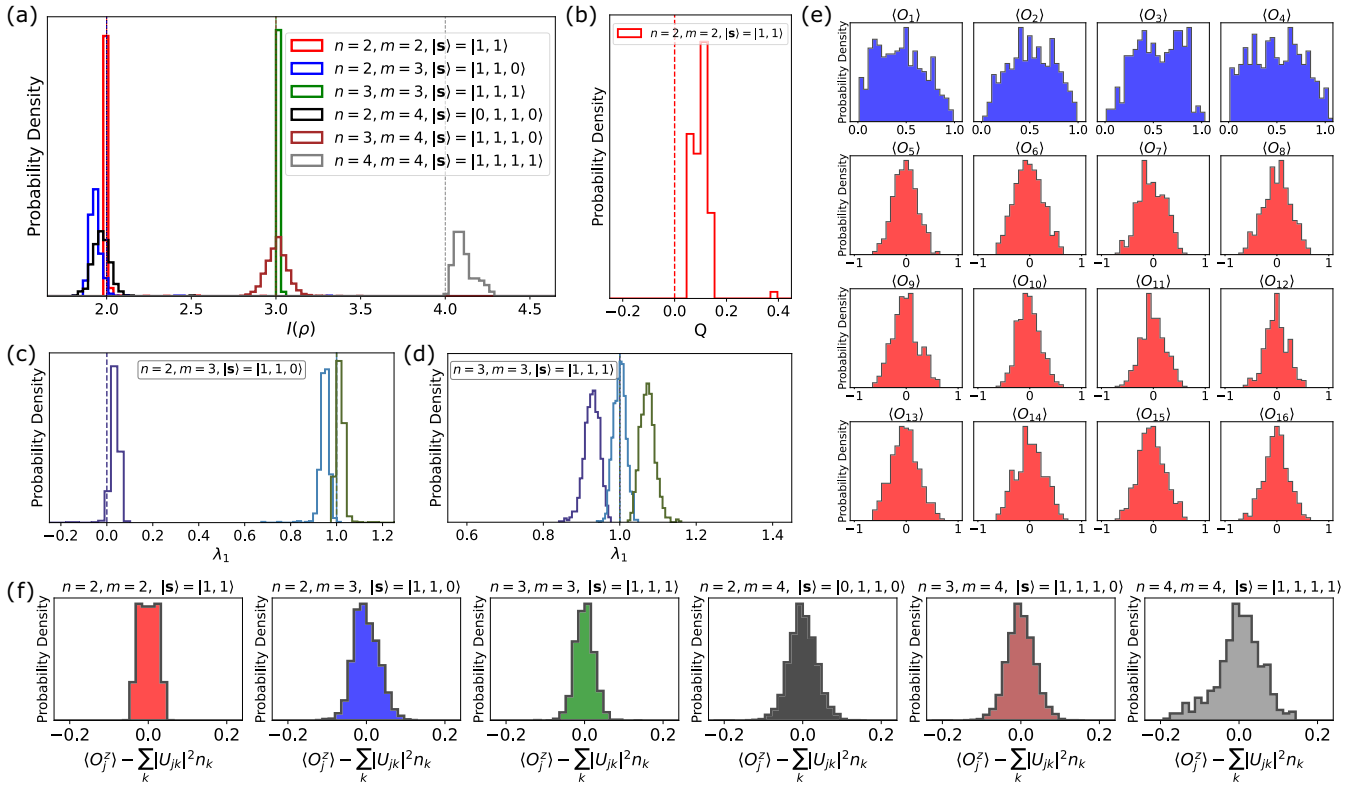


FIG. 3. Experimental distribution of the measured Lie algebraic quantities: (a) Invariance of the quantity $I(\rho)$, measured at the output of a $m \times m$ Haar-random linear optical evolution, with a given Fock state $|\boldsymbol{s}\rangle$ featuring $n$ photons distributed over $m$ modes. The higher deviation from the expected values for the $n = 4$ case has to be attributed to the need of a more complex measurement configuration leading to a larger impact of experimental imperfections. (b)–(d) Spectral properties of the density operator $\rho_T$ as defined in Eq. (4). Specifically, in panel (b), we analyze the principal component $Q$ of the infinite-cardinality spectrum of the operator $\rho_T$ in the $m = 2$ modes configuration; in panels (c)–(d), we show the eigenvalues $\{\lambda_1^j\}$ of the first block diagonal element of $\rho_T$ in the $m = 3$ configuration, with $n = \{2, 3\}$ photons. As detailed in the Supplemental Material [54], these eigenvalues are exactly those of the coherency matrix $\mathbf{\Gamma}^{(1)}$. (e) Histograms of the measured expectation values of the Lie observables $\langle O_i \rangle_\rho$ for the configuration with $m = 4$ and $n = 2$. We denote with different colors histograms for $\langle O_j^z \rangle_\rho$ (blue) and for $\langle O_{jk}^{x,y} \rangle_\rho$ (red). This shows that the invariance arises not at the level of the individual expectation values $\mathrm{Tr}(\rho O_i)$, but only when considering their complete combination $I(\rho)$ as defined in Eq. (2). (f) Histograms of the quantity $\langle O_j^z \rangle_\rho - \sum_k |U_{jk}|^2 n_k$, obtained from experimental data across different configurations. Here, $U$ represents the probed unitary transformations, while $\{n_k\}$ denotes the input state occupation numbers. For each color-coded configuration, the vertical lines indicate the theoretical expectations for the corresponding Lie invariant [panel (a)] or spectral quantities [panels (b)–(d)].

experimentally measured values of $I_{\mathrm{exp}}(\rho)$ and the theoretically expected one can be explained by taking into account typical experimental imperfections of the apparatus, leading to small errors in the implementation of the observables for the Lie invariant measurement, or a miscalibration of the pseudo photon number resolving setup (see the Supplemental Material [54] for a qualitative numerical analysis of such effects).

Interestingly, the expectation value of the photon number operator in a given mode after a linear optical evolution $\tilde{U}$ satisfies the relation $\langle n_j \rangle = \sum_k |\tilde{U}_{jk}|^2 n_k$, where $n_k$ is the photon number in the $j$th input of the interferometer [62], as discussed in the Supplemental Material [54]. Since the expectation values of all observables are reconstructed from measured values of $\langle n_j \rangle$, all the measured quantities are functions of initial occupation numbers and unitary moduli of the optical evolution matrix, and thus they are not dependent on multiphoton distinguishability. However, as shown in Fig. 3(e), each single expectation value $\langle O_i \rangle$ does distribute in the whole range $[-1, +1]$. Only by combining them via Eq. (2), a Lie algebraic invariant is obtained. Given the aforementioned experimental imperfections, these terms can further contribute as a source of uncertainty in the estimation of $I_{\mathrm{exp}}(\rho)$. Finally, Fig. 3(f) reports histograms for the measured distributions of the quantity $\langle O_j^z \rangle_\rho - \sum_k |U_{jk}|^2 n_k$. There, in each configuration, the distributions are centered around zero, confirming the theoretical expectation $\langle O_j^z \rangle_\rho = \langle n_j \rangle_\rho = \sum_k |U_{jk}|^2 n_k$. This observation indirectly confirms both that a given transformation is implemented on the device with a high degree of accuracy, and that the cross configurations required to implement mode swapping in the measurement stage are well implemented.

### C. Inference of the spectra of operator $\rho_T$

As a final step we estimate, from the measured experimental data, the spectrum of the density operator as defined in Eq. (4). In the two-mode scenario, it is possible to show (see Supplemental Material [54])

TABLE I. Measured values for the Lie invariant $\boldsymbol{I(\rho)}$, obtained with different configurations corresponding to different inputs $|\boldsymbol{s}\rangle$ with a varying number of photons $n$ and modes $m$. For the $m = 2$ and $m = 3$ scenarios, we also report the measured quantities related to the spectrum of $\rho_T$, which are $Q$ and $\{\lambda_1^j\}$ respectively. In each row, we provide the average and associated standard deviation of each quantity, computed over the total number $n_{\mathrm{U}}$ of dialed linear unitary evolution. We also report the average value of $1 - \mathrm{TD}_{\mathrm{sim}}$, across all unitary transformations and observables for the given configuration, as a measure of the quality of the population reconstruction.

| $(n, m)$ | $\lvert\boldsymbol{s}\rangle$ | $I(\rho)$ | $Q/\{\lambda_1^j\}$ | $n_{\mathrm{U}}$ | $1 - \mathrm{TD}_{\mathrm{sim}}$ |
|---|---|---|---|---|---|
| (2, 2) | $\lvert 1, 1\rangle$ | 2.008(40) | 0.100(38) | 1000 | 0.92(5) |
| (2, 3) | $\lvert 1, 1, 0\rangle$ | 1.936(73) | $\begin{pmatrix}0.035(29)\\0.947(24)\\1.018(32)\end{pmatrix}$ | 500 | 0.91(4) |
| (2, 4) | $\lvert 0, 1, 1, 0\rangle$ | 1.970(57) | | 400 | 0.90(4) |
| (3, 3) | $\lvert 1, 1, 1\rangle$ | 3.012(6) | $\begin{pmatrix}0.927(20)\\1.000(16)\\1.073(19)\end{pmatrix}$ | 1000 | 0.87(5) |
| (3, 4) | $\lvert 1, 1, 1, 0\rangle$ | 3.007(65) | | 1250 | 0.85(4) |
| (4, 4) | $\lvert 1, 1, 1, 1\rangle$ | 4.111(58) | | 120 | 0.81(3) |

that the spectrum of $\rho_T$ is given by $\lambda_n^j = \frac{n}{2}(N_1 + N_2) + j\sqrt{(N_1 - N_2)^2 + 4|R_{12}|^2}$. Here, $j \in \{-\frac{n}{2}, -\frac{n}{2} + 1, \ldots, \frac{n}{2} - 1, \frac{n}{2}\}$; $N_j = \langle n_j\rangle_\rho$ and $R_{jk} = \frac{1}{\sqrt{2}}(\langle O_{jk}^x\rangle_\rho + i\langle O_{jk}^y\rangle_\rho)$. In order to test whether the spectrum of $\rho_T$ is invariant under linear optical evolution, we consider the input Fock state $|\boldsymbol{s}\rangle = |1, 1\rangle$. In the regime with postselected output, the total number of photons $N_1 + N_2$ is conserved, so that the only nontrivial part of the spectrum is given by $Q = \sqrt{(N_1 - N_2)^2 + 4|R_{12}|^2}$. In the Supplemental Material [54], we show that this quantity is related to the norm of the traceless part of the coherency matrix $\boldsymbol{\Gamma}^{(1)}$. Moreover, we show that it is also related to the invariant $I(\rho)$ through the relation $Q^2 = 2I(\rho) - (N_1 + N_2)^2$. This redundancy is expected since if we exclude the total number of photons we have only $m - 1 = 1$ nontrivial independent quantity in the $m = 2$ scenario. Figure 3(b) shows the distribution of the values of $Q$ as obtained from the experimentally measured $N_j$ and $R_{12}$ for $n = m = 2$, which is in agreement with the theoretically expected value $Q_{\mathrm{theo}} = 0$. In the three-mode scenario, the analysis of the eigenvalue problem for the operator $\rho_T$ was restricted to its first block diagonal element, associated with $n = 1$, as detailed in the Supplemental Material [54]. There, we show that the spectra of such subelement is given by the eigenvalues of a $3 \times 3$ Hermitian matrix $M$, which is found to be exactly the complex conjugate of the coherency matrix $\boldsymbol{\Gamma}^{(1)}$ (see Supplemental Material [54]), and thus has the same eigenvalues. This matrix can be constructed via a measurement of $N_j$ and $R_{jk}$ and diagonalized numerically. In Figs. 3(c) and 3(d), we show the distributions for the numerically computed eigenvalues $\{\lambda_1^j\}$ of the matrix $M$—reconstructed from the experimental data for each unitary $U$—for two input state configurations $|1, 1, 0\rangle$ and $|1, 1, 1\rangle$, showing a very good agreement with their expected theoretical values denoted with vertical lines.

Moreover, as shown in Theorem 4 of Ref. [44], one can consider an equivalent set of $m$ invariants under linear optical evolution, defined in terms of the expectation values of the observables $O_i$. Notably, these invariants do not contain more information than those given by the spectrum of $\rho_T$ (or equivalently of the coherency matrix $\boldsymbol{\Gamma}^{(1)}$). These invariants can be experimentally reconstructed without the need for numerical diagonalization, and can also be evaluated for $m = 4$ configurations, as detailed in the Supplemental Material [54].

## IV. DISCUSSION AND OUTLOOK

In this work, we have highlighted the relevance of Lie algebraic invariants in the characterization of the evolution of quantum states within linear optical systems, by means of boson sampling experiments carried out in a wide range of optical configurations. Leveraging a state-of-the-art hybrid photonic platform, we have experimentally validated the invariance of several different observable quantities that characterize the linear optical dynamic of photonic states, and that are derived from the Lie algebra of the linear-optics Hamiltonians. Recalling the formalism of quantum correlation functions, we have shown how these invariants can be related to the conservation of fundamental coherence properties of the state, upon being subject to a linear optical transformation. Our experimental results provide a concrete demonstration that the Lie algebraic framework—which could be regarded purely as an abstract theoretical tool—can be effectively harnessed in real-world photonic quantum information systems. Indeed, we have shown that the Lie algebraic framework—going beyond the typical formalism of bsoson ampling based on the scattering matrices—can be practically applied within a prototypical architecture for photonic quantum computation. This not only offers an alternative lens through which to analyze quantum optical processes but could also lay the groundwork for the development of future benchmarking protocols, tailored to test the linearity of an underlying bosonic dynamic and thus providing insights on where error thresholds are reached [63,64], or for the analysis of photon-based quantum information protocols, to be added to other existing complementary tools.

## ACKNOWLEDGEMENTS

This work was supported by the ERC Advanced Grant No. QU-BOSS (QUantum advantage via nonlinear BOSon Sampling, Grant Agreement No. 884676), the PNRR MUR Project No. PE0000023-NQSTI (Spoke 4 and Spoke 7), and the European Union's Horizon Europe research and innovation program under EPIQUE Project (Grant Agreement No. 101135288). Fabrication of the fully reconfigurable photonic circuit was partially performed at PoliFAB [65], the micro and nanofabrication facility of Politecnico di Milano. F.C. and R.O. would like to thank the PoliFAB staff for valuable technical support.

G.Co., F.C. and R.O. are co-founders of Ephos. The other authors declare no competing interests.

## DATA AVAILABILITY

The data that support the findings of this article are not publicly available. The data are available from the authors upon reasonable request.

[1] P. Kok, W. J. Munro, K. Nemoto, T. C. Ralph, J. P. Dowling, and G. J. Milburn, Linear optical quantum computing with photonic qubits, Rev. Mod. Phys. **79**, 135 (2007).

[2] K. R. Motes, J. P. Olson, E. J. Rabeaux, J. P. Dowling, S. J. Olson, and P. P. Rohde, Linear optical quantum metrology with single photons: Exploiting spontaneously generated entanglement to beat the shot-noise limit, Phys. Rev. Lett. **114**, 170802 (2015).

[3] F. Ewert, M. Bergmann, and P. van Loock, Ultrafast long-distance quantum communication with static linear optics, Phys. Rev. Lett. **117**, 210501 (2016).

[4] S. Slussarenko and G. J. Pryde, Photonic quantum information processing: A concise review, Appl. Phys. Rev. **6**, 041303 (2019).

[5] F. Flamini, N. Spagnolo, and F. Sciarrino, Photonic quantum information processing: A review, Rep. Prog. Phys. **82**, 016001 (2018).

[6] S. Aaronson and A. Arkhipov, The computational complexity of linear optics, in *Proceedings of the 43rdAnnual ACM Symposium on Theory of Computing*, *STOC'11* (ACM, New York, 2011), p. 333.

[7] D. J. Brod, E. F. Galvão, A. Crespi, R. Osellame, N. Spagnolo, and F. Sciarrino, Photonic implementation of boson sampling: A review, Adv. Photon. **1**, 034001 (2019).

[8] A. Lund, A. Laing, S. Rahimi-Keshari, T. Rudolph, J. O'Brien, and T. Ralph, Boson sampling from a Gaussian state, Phys. Rev. Lett. **113**, 100502 (2014).

[9] C. S. Hamilton, R. Kruse, L. Sansoni, S. Barkhofen, C. Silberhorn, and I. Jex, Gaussian boson sampling, Phys. Rev. Lett. **119**, 170501 (2017).

[10] R. Kruse, C. S. Hamilton, L. Sansoni, S. Barkhofen, C. Silberhorn, and I. Jex, Detailed study of Gaussian boson sampling, Phys. Rev. A **100**, 032326 (2019).

[11] U. Chabaud, D. Markham, and A. Sohbi, Quantum machine learning with adaptive linear optics, Quantum **5**, 496 (2021).

[12] N. Spagnolo, D. J. Brod, E. F. Galvão, and F. Sciarrino, Nonlinear boson sampling, npj Quantum Inf. **9**, 3 (2023).

[13] S. Aaronson and L. Chen, Complexity-theoretic foundations of quantum supremacy experiments, in *Proceedings of the 32nd Computational Complexity Conference* (Schloss Dagstuhl–Leibniz-Zentrum fuer Informatik, Dagstuhl, DEU, 2017).

[14] J. Preskill, Quantum computing in the NISQ era and beyond, Quantum **2**, 79 (2018).

[15] T. Heindel, J.-H. Kim, N. Gregersen, A. Rastelli, and S. Reitzenstein, Quantum dots for photonic quantum information technology, Adv. Opt. Photon. **15**, 613 (2023).

[16] T. Giordani, F. Hoch, G. Carvacho, N. Spagnolo, and F. Sciarrino, Integrated photonics in quantum technologies, La Rivista del Nuovo Cimento **46**, 71 (2023).

[17] J. Wang, F. Sciarrino, A. Laing, and M. G. Thompson, Integrated photonic quantum technologies, Nat. Photon. **14**, 273 (2019).

[18] E. Knill, R. Laflamme, and G. J. Milburn, A scheme for efficient quantum computation with linear optics, Nature (London) **409**, 46 (2001).

[19] S. Bartolucci, P. Birchall, H. Bombín, H. Cable, C. Dawson, M. Gimeno-Segovia, E. Johnston, K. Kieling, N. Nickerson, M. Pant, F. Pastawski, T. Rudolph, and C. Sparrow, Fusion-based quantum computation, Nat. Commun. **14**, 912 (2023).

[20] M. A. Broome, A. Fedrizzi, S. Rahimi-Keshari, J. Dove, S. Aaronson, T. C. Ralph, and A. G. White, Photonic boson sampling in a tunable circuit, Science **339**, 794 (2013).

[21] J. B. Spring, B. J. Metcalf, P. C. Humphreys, W. S. Kolthammer, X.-M. Jin, M. Barbieri, A. Datta, N. Thomas-Peter, N. K. Langford, D. Kundys, J. C. Gates, B. J. Smith, P. G. R. Smith, and I. A. Walmsley, Boson sampling on a photonic chip, Science **339**, 798 (2013).

[22] M. Tillmann, B. Dakić, R. Heilmann, S. Nolte, A. Szameit, and P. Walther, Experimental boson sampling, Nat. Photon. **7**, 540 (2013).

[23] A. Crespi, R. Osellame, R. Ramponi, D. J. Brod, E. F. Galvão, N. Spagnolo, C. Vitelli, E. Maiorino, P. Mataloni, and F. Sciarrino, Integrated multimode interferometers with arbitrary designs for photonic boson sampling, Nat. Photon. **7**, 545 (2013).

[24] J. Loredo, M. Broome, P. Hilaire, O. Gazzano, I. Sagnes, A. Lemaitre, M. Almeida, P. Senellart, and A. White, Boson sampling with single-photon Fock states from a bright solid-state source, Phys. Rev. Lett. **118**, 130503 (2017).

[25] Y. He, X. Ding, Z.-E. Su, H.-L. Huang, J. Qin, C. Wang, S. Unsleber, C. Chen, H. Wang, Y.-M. He, X.-L. Wang, W.-J. Zhang, S.-J. Chen, C. Schneider, M. Kamp, L.-X. You, Z. Wang, S. Höfling, C.-Y. Lu, and J.-W. Pan, Time-bin-encoded boson sampling with a single-photon device, Phys. Rev. Lett. **118**, 190501 (2017).

[26] J. Wang, S. Paesani, R. Santagati, S. Knauer, A. A. Gentile, N. Wiebe, M. Petruzzella, J. L. O'Brien, J. G. Rarity, A. Laing, and M. G. Thompson, Experimental quantum Hamiltonian learning, Nat. Phys. **13**, 551 (2017).

[27] H.-S. Zhong, Y. Li, W. Li, L.-C. Peng, Z.-E. Su, Y. Hu, Y.-M. He, X. Ding, W. Zhang, H. Li, L. Zhang, Z. Wang, L. You, X.-L. Wang, X. Jiang, L. Li, Y.-A. Chen, N.-L. Liu, C.-Y. Lu, and J.-W. Pan, 12-photon entanglement and scalable scattershot boson sampling with optimal entangled-photon pairs from parametric down-conversion, Phys. Rev. Lett. **121**, 250505 (2018).

[28] H. Wang, J. Qin, X. Ding, M.-C. Chen, S. Chen, X. You, Y.-M. He, X. Jiang, L. You, Z. Wang, C. Schneider, J. J. Renema, S. Höfling, C.-Y. Lu, and J.-W. Pan, Boson sampling with 20 input photons and a 60-mode interferometer in a $10^{14}$-dimensional Hilbert space, Phys. Rev. Lett. **123**, 250503 (2019).

[29] H.-S. Zhong, *et al.*, Quantum computational advantage using photons, Science **370**, 1460 (2020).

[30] L. S. Madsen, F. Laudenbach, M. F. Askarani, F. Rortais, T. Vincent, J. F. F. Bulmer, F. M. Miatto, L. Neuhaus, L. G. Helt, M. J. Collins, A. E. Lita, T. Gerrits, S. W. Nam, V. D. Vaidya, M. Menotti, I. Dhand, Z. Vernon, N. Quesada, and J. Lavoie, Quantum computational advantage with a programmable photonic processor, Nature (London) **606**, 75 (2022).

[31] Y.-H. Deng, *et al.*, Gaussian boson sampling with pseudo-photon-number-resolving detectors and quantum computational advantage, Phys. Rev. Lett. **131**, 150601 (2023).

[32] F. Hoch, *et al.*, Quantum machine learning with adaptive boson sampling via post-selection, Nat. Commun. **16**, 902 (2025).

[33] G. Rodari, L. Novo, R. Albiero, A. Suprano, C. T. Tavares, E. Caruccio, F. Hoch, T. Giordani, G. Carvacho, M. Gardina, N. D. Giano, S. D. Giorgio, G. Corrielli, F. Ceccarelli, R. Osellame,

N. Spagnolo, E. F. Galvão, and F. Sciarrino, Semi-device independent characterization of multiphoton indistinguishability, PRX Quantum **6**, 020340 (2025).

[34] R. van der Meer, P. Hooijschuur, F. H. Somhorst, P. Venderbosch, M. de Goede, B. Kassenberg, H. Snijders, C. T. Taballione, J. Epping, H. van den Vlekkert, N. Walk, P. W. H. Pinkse, and J. J. Renema, Experimental demonstration of an efficient, semi-device-independent photonic indistinguishability witness, arXiv:2112.00067.

[35] M. Walschaers, J. Kuipers, J.-D. Urbina, K. Mayer, M. C. Tichy, K. Richter, and A. Buchleitner, Statistical benchmark for bosonsampling, New J. Phys. **18**, 032001 (2016).

[36] T. Giordani, F. Flamini, M. Pompili, N. Viggianiello, N. Spagnolo, A. Crespi, R. Osellame, N. Wiebe, M. Walschaers, A. Buchleitner, and F. Sciarrino, Experimental statistical signature of many-body quantum interference, Nat. Photon. **12**, 173 (2018).

[37] S. Aaronson and A. Arkhipov, Bosonsampling is far from uniform, Quantum Info. Comput. **14**, 1383 (2014).

[38] M. C. Tichy, K. Mayer, A. Buchleitner, and K. Mølmer, Stringent and efficient assessment of boson-sampling devices, Phys. Rev. Lett. **113**, 020502 (2014).

[39] A. Crespi, R. Osellame, R. Ramponi, M. Bentivegna, F. Flamini, N. Spagnolo, N. Viggianiello, L. Innocenti, P. Mataloni, and F. Sciarrino, Suppression law of quantum states in a 3D photonic fast fourier transform chip, Nat. Commun. **7**, 10469 (2016).

[40] N. Spagnolo, C. Vitelli, M. Bentivegna, D. J. Brod, A. Crespi, F. Flamini, S. Giacomini, G. Milani, R. Ramponi, P. Mataloni, R. Osellame, E. F. Galvão, and F. Sciarrino, Experimental validation of photonic boson sampling, Nat. Photon. **8**, 615 (2014).

[41] M. Pont, R. Albiero, S. E. Thomas, N. Spagnolo, F. Ceccarelli, G. Corrielli, A. Brieussel, N. Somaschi, H. Huet, A. Harouri, A. Lemaître, I. Sagnes, N. Belabas, F. Sciarrino, R. Osellame, P. Senellart, and A. Crespi, Quantifying n-photon indistinguishability with a cyclic integrated interferometer, Phys. Rev. X **12**, 031033 (2022).

[42] I. Agresti, N. Viggianiello, F. Flamini, N. Spagnolo, A. Crespi, R. Osellame, N. Wiebe, and F. Sciarrino, Pattern recognition techniques for boson sampling validation, Phys. Rev. X **9**, 011013 (2019).

[43] M. L. Goh, M. Larocca, L. Cincio, M. Cerezo, and F. Sauvage, Lie-algebraic classical simulations for quantum computing, Phys. Rev. Res. **7**, 033266 (2025).

[44] P. V. Parellada, V. G. i Garcia, J. J. Moyano-Fernández, and J. C. Garcia-Escartin, Lie algebraic invariants in quantum linear optics, arXiv:2409.12223.

[45] P. V. Parellada, V. G. i Garcia, J. J. Moyano-Fernández, and J. C. Garcia-Escartin, No-go theorems for photon state transformations in quantum linear optics, Results Phys. **54**, 107108 (2023).

[46] J. C. Garcia-Escartin, V. Gimeno, and J. J. Moyano-Fernández, Multiple photon effective Hamiltonians in linear quantum optical networks, Opt. Commun. **430**, 434 (2019).

[47] N. Somaschi, V. Giesz, L. De Santis, J. C. Loredo, M. P. Almeida, G. Hornecker, S. L. Portalupi, T. Grange, C. Antón, J. Demory, C. Gómez, I. Sagnes, N. D. Lanzillotti-Kimura, A. Lemaítre, A. Auffeves, A. G. White, L. Lanco, and P. Senellart, Near-optimal single-photon sources in the solid state, Nat. Photon. **10**, 340 (2016).

[48] P. Senellart, G. Solomon, and A. White, High-performance semiconductor quantum-dot single-photon sources, Nat. Nanotechnol. **12**, 1026 (2017).

[49] G. Corrielli, A. Crespi, and R. Osellame, Femtosecond laser micromachining for integrated quantum photonics, Nanophotonics **10**, 3789 (2021).

[50] C. Pentangelo, F. Ceccarelli, S. Piacentini, R. Albiero, E. Urbinati, N. Di Giano, S. Atzeni, A. Crespi, and R. Osellame, Universal photonic processors fabricated by femtosecond laser writing, in *Integrated Optics: Devices, Materials, and Technologies XXVI* (SPIE, San Francisco, California, 2022), p. 19.

[51] C. Pentangelo, N. Di Giano, S. Piacentini, R. Arpe, F. Ceccarelli, A. Crespi, and R. Osellame, High-fidelity and polarization-insensitive universal photonic processors fabricated by femtosecond laser writing, Nanophotonics **13**, 2259 (2024).

[52] W. R. Clements, P. C. Humphreys, B. J. Metcalf, W. S. Kolthammer, and I. A. Walmsley, Optimal design for universal multiport interferometers, Optica **3**, 1460 (2016).

[53] R. A. Campos, B. E. A. Saleh, and M. C. Teich, Quantum-mechanical lossless beam splitter: SU(2) symmetry and photon statistics, Phys. Rev. A **40**, 1371 (1989).

[54] See Supplemental Material at http://link.aps.org/supplemental/10.1103/7961-hg2q for further theoretical derivations, details on the experiment, and data analysis, which also includes Refs. [66–72].

[55] C. Fabre and N. Treps, Modes and states in quantum optics, Rev. Mod. Phys. **92**, 035005 (2020).

[56] R. J. Glauber, The quantum theory of optical coherence, Phys. Rev. **130**, 2529 (1963).

[57] G. Rodari, C. Fernandes, E. Caruccio, A. Suprano, F. Hoch, T. Giordani, G. Carvacho, R. Albiero, N. D. Giano, G. Corrielli, F. Ceccarelli, R. Osellame, D. J. Brod, L. Novo, N. Spagnolo, E.F. Galvão, and F. Sciarrino, Experimental observation of counter-intuitive features of photonic bunching, arXiv:2410.15883.

[58] G. Rodari, F. Hoch, A. Suprano, T. Giordani, E. Negro, G. Carvacho, N. Spagnolo, E. F. Galvão, and F. Sciarrino, Polarization-encoded photonic quantum-to-quantum bernoulli factory based on a quantum dot source, Sci. Adv. **10**, eado6244 (2024).

[59] H. Ollivier, I. Maillette de Buy Wenniger, S. Thomas, S. C. Wein, A. Harouri, G. Coppola, P. Hilaire, C. Millet, A. Lemaître, I. Sagnes, O. Krebs, L. Lanco, J. C. Loredo, C. Antón, N. Somaschi, and P. Senellart, Reproducibility of high-performance quantum dot single-photon sources, ACS Photon. **7**, 1050 (2020).

[60] M. Pont, G. Corrielli, A. Fyrillas, I. Agresti, G. Carvacho, N. Maring, P.-E. Emeriau, F. Ceccarelli, R. Albiero, P. H. Dias Ferreira, N. Somaschi, J. Senellart, I. Sagnes, M. Morassi, A. Lemaître, P. Senellart, F. Sciarrino, M. Liscidini, N. Belabas, and R. Osellame, High-fidelity four-photon GHz states on chip, npj Quantum Inf. **10**, 50 (2024).

[61] R. Albiero, C. Pentangelo, M. Gardina, S. Atzeni, F. Ceccarelli, and R. Osellame, Toward higher integration density in femtosecond-laser-written programmable photonic circuits, Micromachines **13**, 1145 (2022).

[62] K. Mayer, M. C. Tichy, F. Mintert, T. Konrad, and A.

Buchleitner, Counting statistics of many-particle quantum walks, Phys. Rev. A **83**, 062307 (2011).

[63] A. Leverrier and R. Garcia-Patron, Analysis of circuit imperfections in boson sampling, Quantum Inf. Comput. **15**, 0489 (2015).

[64] A. Arkhipov, Bosonsampling is robust against small errors in the network matrix, Phys. Rev. A **92**, 062326 (2015).

[65] https://www.polifab.polimi.it/.

[66] D. C. Kay, *Schaum's Outline of Theory and Problems of Tensor Calculus* (McGraw-Hill, 1988).

[67] A. K. Nowak, S. L. Portalupi, V. Giesz, O. Gazzano, C. Dal Savio, P.-F. Braun, K. Karrai, C. Arnold, L. Lanco, I. Sagnes, A. Lemaître, and P. Senellart, Deterministic and electrically tunable bright single-photon source, Nat. Commun. **5**, 3240 (2014).

[68] O. Gazzano, S. Michaelis de Vasconcellos, C. Arnold, A. Nowak, E. Galopin, I. Sagnes, L. Lanco, A. Lemaître, and P. Senellart, Bright solid-state sources of indistinguishable single photons, Nat. Commun. **4**, 1425 (2013).

[69] U. M. Titulaer and R. J. Glauber, Correlation functions for coherent fields, Phys. Rev. **140**, B676 (1965).

[70] L. Qi, Eigenvalues and invariants of tensors, J. Math. Anal. Appl. **325**, 1363 (2007).

[71] L.-B. Cui, C. Chen, W. Li, and M. K. Ng, An eigenvalue problem for even order tensors with its applications, Linear Multilinear Algebra **64**, 602 (2015).

[72] K. E. Cahill and R. J. Glauber, Ordered expansions in boson amplitude operators, Phys. Rev. **177**, 1857 (1969).